Robotica (2011) volume 29, pp. 571–579. © Cambridge University Press 2010
doi:10.1017/S0263574710000421

A worm-inspired new spatial hyper-redundant manipulator

Jaime Gallardo-Alvarado*, Raúl Lesso-Arroyo and J. Santos García-Miranda

Instituto Tecnológico de Celaya, Department of Mechanical Engineering, Av. Tecnológico y García Cubas, 38010 Celaya, GTO, Mexico

(Received in Final Form: July 16, 2010. First published online: August 13, 2010)

SUMMARY

In this work a novel spatial hyper-redundant manipulator inspired in the motions of the worms is introduced. The displacement analysis is presented in a semi-closed form solution, whereas the velocity and acceleration analyses are carried out by means of the theory of screws. Among typical applications of most hyper-redundant manipulators, interesting biomechanical applications such as the simulation of the motion of the spine are available for this new *artificial worm*.

KEYWORDS: Human biomechanics; Novel applications of robotics; Parallel manipulators; Redundant manipulators; Space kinematics.

1. Introduction

As pointed out by Chirikjian,[1] "The term hyper-redundant refers to robotic manipulators and mobile robots with a very large, possibly infinite, number of actuable degrees of freedom. These robots are analogous in morphology and operation to snakes, worms, elephant trunks, and tentacles." This concept is here adopted in order to develop a new manipulator provided with an optional number of extra degrees of freedom; however, it is important to recognize that due to the emergence of several branches approaching this topic, such terminology was redefined may be with the purpose to identify the different ways to obtain the desired hyper-redundancy, e.g. as it is correctly noted by one of the reviewers: "Trunks and tentacles are continuum systems while snakes are hyper redundant mechanical systems. Worms are muscular hydrostatic and are also not hyper redundant mechanical systems." The authors agree that it is necessary to unify the terminology and it is worth mentioning that IFToMM had made significative advances[2] in the subject; however, the simplest concept of hyper-redundant manipulator[3] as a robot with numerous independent degrees of freedom to perform a task introduced almost two decades ago will be used in this paper.

Examples of the performance of redundant manipulators can be found in the nature itself, giving birth to several hyper-redundant manipulators with suggestive names like tentacle,[4] serpentine,[5] snake,[6] or elephant's trunk.[7] Furthermore, considering that a worm is a terrestrial locomotion system without active legs and wheels producing undulatory motions, then a worm can be an inspiration to develop new hyper-redundant manipulators. Certainly, by observing worm motions it is possible to note complicated internal motions yielding sophisticated undulatory trajectories that however are modeled considering only one dominant linear dimension.[8–10]

The benefits of hyper-redundancy kinematics are well studied in quite different scientific communities. Modeling the motions of human body is an opportunity to introduce hyper-redundant manipulators. For example, simulating the kinematics of the spine is a challenging task due to the complexity of several interconnected bodies that form a larger locomotion system. It is remarkable how this subject has attracted the attention of many researchers. Using basic biomechanics, individual segmental range of motions was quantified for all spinal levels by Panjabi and White.[11] Dimnet *et al.*[12] reported a technique, based on lateral-view-X-ray, to determine parameters for describing the centers of rotation and curvature of the spine. Gracovetsky and Farfan[13] proposed a novel theory based on the mechanical behavior of intervertebral joints capable of computing both spinal motions and muscular actions. By means of the technique of videofluoroscopy, Cholewicki and MacGill[14] studied the kinematics of the lumbar spine. Yoganandan *et al.*[15] determined the kinematic response of the lumbar spine using instrumented transpedicular screws and plates. It is well-known that a structure is any assemblage of materials that is intended to sustain loads, a strong argument to simulate the spine, in that way Levin[16] proposes tensegrity structures to simulate the kinematics of the spine. Willems *et al.*[17] provided preliminary information about the spatial kinematics of the thoracic spine *in vivo*. Faber *et al.*[18] proposed a method to compute Euler's angles of rotation of a body segment during locomotion and applied it to *in vivo* spinal kinematics. Garcia and Ravani[19] presented a biomechanical evaluation of whiplash injury potential during the initial extension motion of the head in a rear-end collision in which a four-segment dynamic model is developed in the sagittal plane for the analysis that is available for the cervical spine. In order to demonstrate *in vivo* intervertebral-coupled motions of the upper cervical spine, Yoshikawa *et al.*[20] studied the spatial kinematics of the upper cervical spine during head rotation using three-dimensional magnetic resonance imaging (MRI) in healthy volunteers. Ziddiqui *et al.*[21] investigated the sagittal

* Corresponding author. E-mail: gjaime@itc.mx

kinematics *in vivo* of the lumbar spine at the instrumented level. Ishii *et al.*[22] studied the spatial kinematics of the cervical spine during lateral bending while Konz *et al.*[23] investigated the spatial kinematics of spinal during walking. Chanceya *et al.*[24] determined the center of rotation of the upper cervical considering pure bending. Gill *et al.*[25] examined the effect of changes in horizontal lift distance on the amount of flexion in different spine regions according to different lift styles. In order to approach the so-called shaken baby syndrome, recently Jones *et al.*[26] proposed a methodology for the kinematic analysis of infant spine. Finally, Iqbal and Roy[27] introduced a planar four-segment neuromusculoskeletal model consisting of the ankle, knee, and hip to analyze the dynamic stability and control in a multisegment biomechanical model. Most of the contributions above cited require experimental resources, so cheap and practical mathematical tools, such as the theory of screws, can be used in order to validate/improve these works. Consider, for instance, that Zhu *et al.*[28] proposed some parallel manipulators capable of simulating, by means of the theory of screws, the finite kinematics at the end of the spinal column. Mobile robots are another interesting application of hyper-redundancy kinematics such as the development of hybrid robots devoted to search and rescue tasks.[29]

In this paper, a novel spatial hyper-redundant manipulator (SHRM) inspired by the motions of the worms is introduced. An application of the proposed SHRM discussed herein may include devices for high manipulability in the context of space robotics, obstacle avoidance ability, and biomechanical applications such as the kinematic analysis of the spine. The forward displacement analysis of the proposed SHRM is presented in a semi-closed form solution that allows to compute all the feasible configurations of the proposed SHRM, given the generalized coordinates of the spatial mechanism. Thereafter, the velocity and acceleration analyses are carried out using the theory of screws. Simple and compact expressions are derived here for solving the infinitesimal kinematics of the SHRM by applying the concept of reciprocal screws. Note that the kinematic analysis of a hyper-redundant manipulator is a rather complicated task. This subject has been approached by means of a continuous *backbone curve* which contains essential macroscopic geometric features of the desired motions.[30–32] Finally, a numerical example which consists of solving the forward displacement, velocity, and acceleration analyses of an SHRM built with four modules is included.

2. Description of the Proposed Hyper-Redundant Manipulator

The proposed hyper-redundant manipulator consists of an optional number of identical redundant parallel manipulators with autonomous motions assembled in series connection; see Fig. 1, where n is called *the output platform*, k and $k-1$ are two consecutive platforms, and 0 is the fixed platform.

The base module of the proposed SHRM consists of two platforms, for instance labeled 1 and 0, connected each other by means of a spherical parallel manipulator (SPM) and a redundant planar parallel manipulator (RPPM). Evidently,

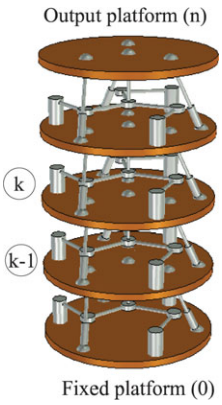

Fig. 1. The proposed hyper-redundant manipulator.

the position and orientation of body 1 with respect to body 0 are controlled independently by means of the SPM and the RPPM, respectively. Hence, the base module can be considered as a decoupled robot. Clearly, the kinematics of a decoupled robot is simpler than the generated in a parallel manipulator with coupled motions over the moving platform.[33–36]

The SPM is a three degrees of freedom parallel manipulator with limbs of the type Spherical + Prismatic + Spherical (SPS), where the prismatic joints have the privilege to be considered as the active kinematic pairs of the SPM. On the other hand, the RPPM is a planar mechanism with limbs of the type Revolute + Revolute + Revolute + Spherical (RRRS). Since the role of the RPPM is to control the position of one point of body 1, for simplicity its geometric center, only two generalized coordinates are necessary to meet this goal; however, the RPPM is conveniently provided with an extra limb in order to give each module the potential possibility to avoid or to escape from possible singularities by actuating the corresponding additional kinematic chain, which under normal conditions of operation plays the role of a simple passive limb. Thus, the base module is a redundant five degrees of freedom decoupled robot with a parallel architecture, three rotations and two translations available for one platform with respect to the other.

Finally, note the great similarity of the proposed SHRM with the spine. Certainly, the simulation of the kinematics of the spine by means of parallel manipulators is a real possibility; see for instance Walker and Dickey[37] and Zhu *et al.*[28,38]

3. Finite Kinematics

Let $OXYZ$ be a reference frame attached at the fixed platform and let $oxyz$ be a reference frame attached at the output platform. The statement of the displacement analysis of the SHRM is as follows: Given the instantaneous generalized coordinates of the SHRM, compute the feasible locations that the output platform can reach with respect to the fixed platform expressed in the global reference frame $OXYZ$.

As an initial step, first, the displacement analysis of the parallel manipulator containing platforms 1 and 0, namely the base module, is presented. Later, the displacement analysis of the SHRM is computed by applying recursively the

https://doi.org/10.1017/S0263574710000421 Published online by Cambridge University Press

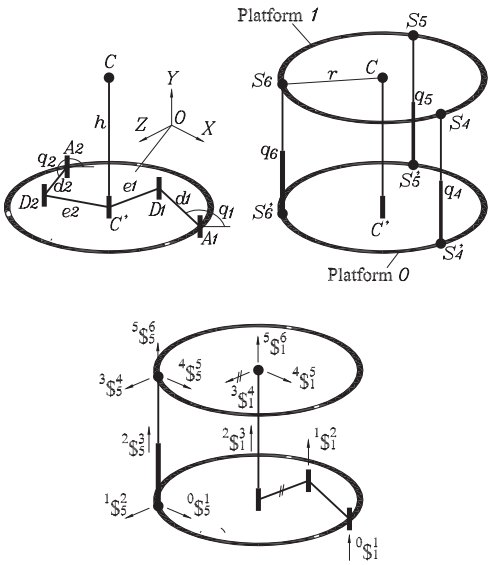

Fig. 2. The base module and its geometric scheme.

expressions thus obtained. To this end, subchains 1 and 2 are chosen as the active limbs of the 3-RRR parallel manipulator. Furthermore, in order to simplify the displacement analysis, the global reference frame OXYZ is placed in such a way that the X and Z axes are located in the plane formed by the points $A_i (i = 1, 2, 3)$, which denote the nominal positions of the revolute joints attached at the fixed platform; see Fig. 2.

To compute the coordinates of point $C' = (C_X, 0, C_Z)$, it immediately emerges that

$$(\boldsymbol{C}' - \boldsymbol{D}_i) \bullet (\boldsymbol{C}' - \boldsymbol{D}_i) - e_i^2 = 0, \quad i = 1, 2 \tag{1}$$

where $\boldsymbol{C}'$ and $\boldsymbol{D}_i$ denote the position of points C' and D_i, respectively. On the other hand, subchain 3 is a passive element and therefore does not affect the position of point C'. Subchain 3 is used as an active element if, and only if, the 3-RRR redundant planar parallel manipulator is at a singular configuration, if any.

From expressions (1) a linear equation with two unknowns, C_X and C_Z, is immediately obtained by subtracting each other the two equations given in (1). Solving this equation for C_X or C_Z and substituting it in any of the expressions (1), a quadratic equation for computing the remaining unknown is generated. Finally, the center of platform 1, point C, results in $C = (C_X, h, C_Z)$. This type of solution is called a closed-form solution, and clearly in this case two different poses are available for platform 1, with respect to platform 0, given a set of generalized coordinates $\{q_1, q_2\}$.

In what follows, the coordinates of points $S_i = (X_i, Y_i, Z_i)$ $i = 4, 5, 6$, denoting the centers of the corresponding spherical joints attached to platform 1, are computed using simple geometric procedures.

It is evident that the center C of the triangle $\Delta S_4 S_5 S_6$ gives the following closure equation:

$$(\boldsymbol{S}_4 + \boldsymbol{S}_5 + \boldsymbol{S}_6)/3 = \boldsymbol{C}, \tag{2}$$

where $\boldsymbol{S}_i (i = 4, 5, 6)$ denotes the position vector of the ith point $S_i (i = 4, 5, 6)$. Furthermore, the extendible limbs must satisfy the following kinematic constraint equations:

$$(\boldsymbol{S}_i - \boldsymbol{S}_i') \bullet (\boldsymbol{S}_i - \boldsymbol{S}_i') = q_i^2, \quad i = 4, 5, 6, \tag{3}$$

where the vector $\boldsymbol{S}_i' (i = 4, 5, 6)$ denotes the position of the point $S_i' (i = 4, 5, 6)$ associated with the corresponding spherical joint attached at the fixed platform.

Finally, three compatibility expressions can be written as

$$(\boldsymbol{S}_i - \boldsymbol{C}) \bullet (\boldsymbol{S}_i - \boldsymbol{C}) = r^2, \quad i = 4, 5, 6 \tag{4}$$

where r is the *radius* of platform 1.

Subtracting Eqs. (3) and (4), it follows that

$$2\boldsymbol{S}_i \bullet (\boldsymbol{C} - \boldsymbol{S}_i') + \boldsymbol{S}_i \bullet \boldsymbol{S}_i' - \boldsymbol{C}_i \bullet \boldsymbol{C}_i - q_i^2 + r^2 = 0, \quad i = 4, 5, 6. \tag{5}$$

Expressions (2) and (5) represent a linear system of six equations in nine unknowns. Solving (2) and (5) in terms of the unknowns X_4, Y_5, and Z_6 and substituting it into Eq. (3) a higher non-linear system of three equations results in

$$\left.\begin{aligned} &k_1 X_4^2 Y_5^2 + k_2 X_4^2 Y_5 + k_3 X_4 Y_5^2 + k_4 X_4 Y_5 \\ &\quad + k_5 X_4 + k_6 Y_5 + k_7 = 0 \\ &k_1' X_4^2 Z_6^2 + k_2' X_4^2 Z_6 + k_3' X_4 Z_6^2 + k_4' X_4 Z_6 \\ &\quad + k_5' X_4 + k_6' Z_6 + k_7' = 0 \\ &k_1'' Y_5^2 Z_6^2 + k_2'' Y_5^2 Z_6 + k_3'' Y_5 Z_6^2 + k_4'' Y_5 Z_6 \\ &\quad + k_5'' Y_5 + k_6'' Z_6 + k_7'' = 0 \end{aligned}\right\} \tag{6}$$

where the coefficients k_*, k_*', and k_*'' are computed given the parameters, including of course the center of platform 1, and generalized coordinates of the spherical parallel manipulator. Expressions (6) are solved by using recursively the Sylvester dialytic elimination method (Innocenti and Parenti-Castelli,[39] Tsai,[40] Gallardo-Alvarado *et al.*[41]), yielding a semi-closed form solution. With this procedure, 16 possible locations, including reflected solutions, of platform 1 with respect to platform 0 are available. Furthermore, considering that two different locations are available for point C, platform 1 can reach 32 different locations or poses with respect to platform 0.

Once the coordinates of the points $S_i (i = 4, 5, 6)$ are computed, the rotation matrix ${}^0\mathbf{R}^1$ of body 1 with respect to body 0 can be obtained, see Gallardo-Alvarado *et al.*,[42] as

$${}^0\mathbf{R}^1 = [\hat{u}_X \quad \hat{u}_Y \quad \hat{u}_Z], \tag{7}$$

where the unit vectors $\hat{u}_*$ are given by

$$\left.\begin{aligned} \hat{u}_Z &= \frac{(\boldsymbol{S}_3 - \boldsymbol{S}_2) \times (\boldsymbol{S}_1 - \boldsymbol{S}_2)}{\|(\boldsymbol{S}_3 - \boldsymbol{S}_2) \times (\boldsymbol{S}_1 - \boldsymbol{S}_2)\|} \\ \hat{u}_X &= \frac{(\boldsymbol{S}_1 - \boldsymbol{C} + \lambda(\boldsymbol{S}_3 - \boldsymbol{S}_1))}{\|\boldsymbol{S}_1 - \boldsymbol{C} + \lambda(\boldsymbol{S}_3 - \boldsymbol{S}_1)\|} \\ \hat{u}_Y &= \hat{u}_Z \times \hat{u}_X \end{aligned}\right\} \tag{8}$$

and the scalar λ is computed according to the known vectors $\boldsymbol{S}_3$ and $\boldsymbol{S}_1$. It must be noted that Eq. (7) requires that $\boldsymbol{C}' - \boldsymbol{S}_i' = \boldsymbol{C} - \boldsymbol{S}_i (i = 4, 5, 6)$, otherwise the rotation between these vectors should be considered in (7).

https://doi.org/10.1017/S0263574710000421 Published online by Cambridge University Press

It is straightforward to show that the method to compute the rotation matrix ${}^0\mathbf{R}^1$ can be applied recursively to find the rotation matrix of any moving platform k of the SHRM with respect to the fixed platform, matrix ${}^0\mathbf{R}^k$, including of course the output platform n. In fact, clearly

$$ {}^0\mathbf{R}^k = {}^0\mathbf{R}^1\ {}^1\mathbf{R}^2 \ldots {}^{k-1}\mathbf{R}^k, \quad k = 1, 2, \ldots, n. \tag{9} $$

Furthermore, the homogeneous transformation matrix ${}^0\mathbf{T}^1$ of body 1 with respect to body 0 is given by

$$ {}^0\mathbf{T}^1 = \begin{bmatrix} {}^0\mathbf{R}^1 & \boldsymbol{C} \\ 0_{1\times 3} & 1 \end{bmatrix}. \tag{10} $$

Thereafter, the transformation matrix between any moving platform k of the SHRM and the fixed platform is obtained as follows:

$$ {}^0\mathbf{T}^k = {}^0\mathbf{T}^1\ {}^1\mathbf{T}^2\ \ldots\ {}^{k-1}\mathbf{T}^k \quad k = 1, 2, \ldots, n. \tag{11} $$

Considering that 32 different solutions, including reflected solutions, are available for the forward displacement analysis of each module, if the SHRM is built with n modules then the output platform can reach 32^n different locations with respect to the fixed platform, without doubt a significative number of possible poses of the body n that shows the extraordinary manipulability of the proposed SHRM. Finally, it is straightforward to show that the coordinates of any point attached at the output platform, expressed in the global reference frame OXYZ, can be computed by expression (11).

4. Infinitesimal Kinematics

The mathematical tool to approach the velocity and acceleration analyses is the theory of screws, and following the trend of Section 3, first, the infinitesimal kinematics of the base module is presented.

4.1. Velocity analysis

Consider the base module which contains platforms 1 and 0, and let ${}^0\boldsymbol{V}^1_{P1} = [{}^0\omega^1; {}^0\boldsymbol{v}^1_{P1}]^{\mathrm{T}}$ be the velocity state, or twist about a screw,[43] of body 1 with respect to body 0, where ${}^0\omega^1$ and ${}^0\boldsymbol{v}^1_{P1}$ are the angular and linear velocities, respectively, of body 1 with respect to body 0 so that the subscript $P1$ denotes a point of body 1 that is instantaneously coincident with a point fixed at the local reference frame, for simplicity $P1$ is chosen at the origin of the global reference frame OXYZ. Then, the velocity state can be written in screw form, the corresponding model of the infinitesimal screws is depicted in Fig. 2, for any of the limbs, as

$$ {}_0\omega^i_1\ {}^0\$^1_i + {}_1\omega^i_2\ {}^1\$^2_i + \cdots + {}_5\omega^i_6\ {}^5\$^6_i = {}^0\boldsymbol{V}^1_{P1} \qquad i = 1, 2, \ldots, 6 \tag{12} $$

or

$$ \mathbf{J}_i \Omega_i = {}^0\boldsymbol{V}^1_{P1}, \tag{13} $$

where $\mathbf{J}_i = [{}^0\$^1_i; {}^1\$^2_i; {}^2\$^3_i; {}^3\$^4_i; {}^4\$^5_i; {}^5\$^6_i]$ is the screw-coordinate Jacobian matrix of the ith limb and $\Omega_i = [{}_0\omega^i_1; {}_1\omega^i_2; {}_1\omega^i_2; {}_2\omega^i_3; {}_3\omega^i_4; {}_4\omega^i_5; {}_5\omega^i_6]^{\mathrm{T}}$ is a matrix containing the joint velocity rates of the ith leg. Note that the joint velocity rates $\{{}_0\omega^1_1 = \dot{q}_1, {}_0\omega^2_1 = \dot{q}_2, {}_2\omega^1_3 = \dot{q}_4, {}_2\omega^2_3 = \dot{q}_5, {}_0\omega^1_1 = \dot{q}_6\}$ have the privilege to be considered as the active kinematic pairs of the base module. Furthermore, the screws ${}^2\$^3_i (i = 1, 2)$ are elements associated with fictitious prismatic pairs in which evidently ${}_2\omega^1_3 = {}_2\omega^2_3 = 0$. These fictitious elements are included only for the sake of completeness of an algebraic requirement, specifically for completing the rank of the Jacobian matrix of limbs 1 and 2.

The inverse velocity analysis (IVA), a necessary task to approach the acceleration analysis, consists of finding the joint velocity rates of the limbs of the base module, given the velocity state of platform 1 with respect to platform 0. The IVA is computed directly from Eq. (13) as

$$ \Omega_i = \mathbf{J}_i^{-1}\ {}^0\boldsymbol{V}^1_{P1}. \tag{14} $$

On the other hand, the forward velocity analysis (FVA) consists of finding the velocity state ${}^0\boldsymbol{V}^1_{P1}$ of body 1 with respect to body 0 given a set of active joint velocity rates $\{\dot{q}_1, \dot{q}_2, \dot{q}_4, \dot{q}_5, \dot{q}_6\}$. The FVA is simplified considerably by applying the concept of reciprocal screw. To this end, note that the screw ${}^3\$^4_1$ is reciprocal to all the screws of limb 1, except the screw ${}^0\$^1_1$, which is associated with the active joint velocity rate $\dot{q}_1$. Therefore, the application of the Klein form[1] of screw ${}^3\$^4_1$ with both sides of the corresponding Eq. (12), the reduction of terms leads to

$$ \left\{{}^3\$^4_1; {}^0\boldsymbol{V}^1_{P1}\right\} = \dot{q}_1 \left\{{}^3\$^4_1; {}^0\$^1_1\right\}, \tag{15} $$

similarly, from limb 2 it follows that

$$ \left\{{}^3\$^4_2; {}^0\boldsymbol{V}^1_{P1}\right\} = \dot{q}_2 \left\{{}^3\$^4_2; {}^0\$^1_2\right\}. \tag{16} $$

Furthermore, the screws ${}^5\$^6_4$, ${}^5\$^6_5$, and ${}^5\$^6_6$ are reciprocal to all the revolute joints in the same limb. Therefore,

$$ \left\{{}^5\$^6_i, {}^0\boldsymbol{V}^1_{P1}\right\} = \dot{q}_i, \quad i = 4, 5, 6. \tag{17} $$

In order to satisfy an algebraic requirement, note that the screw ${}^5\$^6_1$ is reciprocal to all the screws of limb 1 and, therefore, one can obtain

$$ \left\{{}^5\$^6_1, {}^0\boldsymbol{V}^1_{P1}\right\} = 0. \tag{18} $$

Casting Eqs. (15)–(18) into a matrix–vector form, a compact velocity expression is formulated as follows:

$$ \mathrm{J}^{\mathrm{T}}\ \Delta\ {}^0\boldsymbol{V}^1_{P1} = \left[\dot{q}_1\left\{{}^3\$^4_1; {}^0\$^1_1\right\}; \dot{q}_2\left\{{}^3\$^4_2; {}^0\$^1_2\right\}; \dot{q}_4; \dot{q}_5; \dot{q}_6; 0\right]^{\mathrm{T}}, \tag{19} $$

where $\mathbf{J} = [{}^3\$^4_1; {}^3\$^4_2; {}^5\$^6_4; {}^5\$^6_5; {}^5\$^6_6; {}^5\$^6_1]$ is the active screw-coordinate Jacobian matrix of the base module and $\Delta = \left[\begin{smallmatrix} \mathbf{O} & \mathbf{I} \\ \mathbf{I} & \mathbf{O} \end{smallmatrix}\right]$ is an operator of polarity which is a 6×6 matrix defined by the identity matrix $\mathbf{I}$ and the zero matrix $\mathbf{O}$.

[1] Let $\$_1 = (\hat{s}_1, \boldsymbol{s}_{O1})$ and $\$_2 = (\hat{s}_2, \boldsymbol{s}_{O2})$ be two elements of the Lie algebra $e(3)$, which is isomorphic to screw theory, then the Klein form, $\{*; *\}$, is defined as follows:

$$ \{\$_1; \$_2\} = \hat{s}_1 \bullet \boldsymbol{s}_{O2} + \hat{s}_2 \bullet \boldsymbol{s}_{O1}. $$

It is said that the screws $\$_1$ and $\$_2$ are reciprocal if $\{\$_1; \$_2\} = 0$.

https://doi.org/10.1017/S0263574710000421 Published online by Cambridge University Press

Since the velocity state satisfies the conditions of helicoidal vector fields, see Gallardo-Alvarado *et al.*,[44] it is possible to write

$$ {}^0\boldsymbol{V}_O^1 = \begin{bmatrix} {}^0\omega^1 \\ {}^0\boldsymbol{v}_{P1}^1 + {}^0\omega^1 \times \boldsymbol{r}_{O/P1} \end{bmatrix}, \tag{20} $$

where $\boldsymbol{r}_{O/P1}$, known as the vector of the helicoidal field, is the position vector of point O with respect to point $P1$. Furthermore, the velocity state between any moving platform k, including the output platform n, and the fixed platform, body 0, can be obtained, see Rico and Duffy,[45] as

$$ {}^0\boldsymbol{V}_O^k = {}^0\boldsymbol{V}_O^1 + {}^1\boldsymbol{V}_O^2 + \cdots + {}^{k-1}\boldsymbol{V}_O^k \quad k = 1, 2, \ldots, n, \tag{21} $$

where each relative velocity state ${}^{k-1}\boldsymbol{V}_O^k (k = 1, \ldots, n)$ is computed, using properly the corresponding reference frames, according to Eqs. (19) and (20).

Finally, once the velocity state of the output platform with respect to the fixed platform is computed, six-dimensional vector ${}^0\boldsymbol{V}_O^n = [{}^0\omega^n; {}^0\boldsymbol{v}_O^n]^{\mathrm{T}}$, the linear velocity of the center of the output platform is obtained using elementary kinematics as follows:

$$ {}^0\boldsymbol{v}_o^n = {}^0\boldsymbol{v}_O^n + {}^0\omega^n \times \boldsymbol{r}_{o/O}, \tag{22} $$

where $\boldsymbol{r}_{o/O}$ is the position vector of the origin of the reference frame oxyz with respect to the origin of the global reference frame OXYZ.

4.2. Singularity analysis

Since the base module is a 3SPS+3RRRS decoupled parallel manipulator, the singularity analysis is approached by analyzing separately the spherical and translational parallel manipulators.

The singularity analysis of the 3SPS parallel manipulator was successfully approached in Alici and Shirinzadeh[46] and, therefore, it is unnecessary to include it here. On the other hand, it is evident that the singularities of the translational parallel manipulator can be investigated by considering it as a 5R closed chain; see Fig. 3. Initially, the manipulator under study is modeled as an open serial chain in which the velocity state of body 5 with respect to body 0 is given by

$$ {}_0\omega_1\,{}^0\$^1 + {}_1\omega_2\,{}^1\$^2 + {}_2\omega_3\,{}^2\$^3 + {}_3\omega_4\,{}^3\$^4 + {}_4\omega_5\,{}^4\$^5 = {}^0\boldsymbol{V}^5, \tag{23} $$

where the screws are reduced to three-dimensional vectors. As demonstrated by Rico *et al.*,[47] in a serial manipulator the screws connecting it to the base link and the end-effector are not responsible to fall or to escape the manipulator from a singular configuration and therefore the joint rates ${}_0\omega_1$ and ${}_4\omega_5$, associated with the active joints q_1 and q_2, respectively, must be disregarded immediately from the analysis, even though they are the motors of the manipulator. On the other hand, if body 5 is joined to body 0, then the open manipulator becomes a closed chain where ${}^0\boldsymbol{V}^5 = \boldsymbol{0}$. Thereafter, Eq. (23)

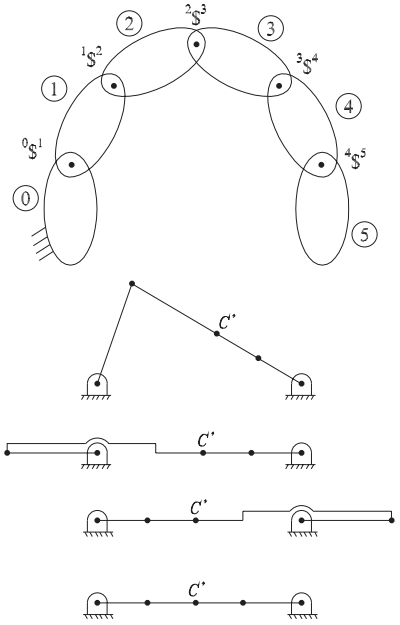

Fig. 3. The 5R manipulator and some of its singular configurations.

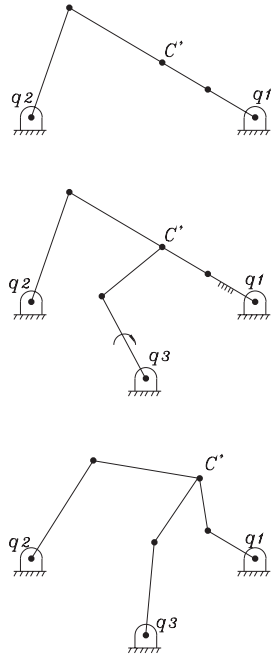

Fig. 4. The 5R manipulator escaping from a singularity.

is rewritten in a matrix–vector form as

$$ \mathbf{J}_s \begin{bmatrix} {}_1\omega_2 \\ {}_2\omega_3 \\ {}_3\omega_4 \end{bmatrix} = -\,{}_0\omega_1\,{}^0\$^1 - {}_4\omega_5\,{}^4\$^5, \tag{24} $$

where $\mathbf{J}_s = [{}^1\$^2, {}^2\$^3, {}^3\$^4]$. In order to solve (24) it is necessary that $\det(\mathbf{J}_s) \neq 0$. In other words, the closed chain is at a singular configuration if the screws ${}^1\$^2$, ${}^2\$^3$, and ${}^3\$^4$ are linearly independent, which implies that $\dim(\mathbf{J}_s) < 3$, which occurs mainly when the revolute joints of such screws are aligned; see Fig. 3.

In what follows, it is shown how the closed chain can escape from a singularity by means of a simple case. To this end, consider the singular configuration depicted in Fig. 4.

https://doi.org/10.1017/S0263574710000421 Published online by Cambridge University Press

In order to escape from the singularity, the following steps are suggested:

(1) Detect the singularity. Since $\det(\mathbf{J}_s)=0$, the closed chain is at a singular configuration.
(2) Lock the revolute joint q_1, e.g. $\dot{q}_1=0$, and unlock q_2 such that this revolute joint becomes a passive element.
(3) Consider the third limb, containing q_3, as an active leg which implies that point C' can move along a circular trajectory.
(4) Since none of the closed chains are at a singular configuration (dealing with the inverse velocity analysis), the motor q_3 can be actuated producing a circular trajectory over point C' eliminating the undesirable alignment of the revolute joints responsible for causing the singularity of the original closed chain.
(5) Finally, once the closed chain is out of the singularity, the motors q_1 and q_2 can recover their roles of active kinematic joints.

4.3. Acceleration analysis

Consider the base module which contains platforms 1 and 0, and let ${}^0\boldsymbol{A}^1_{P1}=[{}^0\dot{\boldsymbol{\omega}}^1;{}^0\boldsymbol{a}^1_{P1}-{}^0\boldsymbol{\omega}^1\times{}^0\boldsymbol{v}^1_{P1}]^{\mathrm{T}}$ be the reduced acceleration state, or accelerator for brevity, of body 1 with respect to body 0, where ${}^0\dot{\boldsymbol{\omega}}^1$ and ${}^0\boldsymbol{a}^1_{P1}$ are the angular and linear accelerations of body 1, respectively, with respect to body 0 taking point $P1$ as the reference pole. Then, the accelerator can be written in screw form, see Rico and Duffy,[45] for any of the limbs as follows:

$$ {}_0\dot{\omega}^i_1\,{}^0\$^1_i+{}_1\dot{\omega}^i_2\,{}^1\$^2_i+\cdots+{}_5\dot{\omega}^i_6\,{}^5\$^6_i+\mathcal{L}_i={}^0\boldsymbol{A}^1_{P1},\quad i=1,2,\ldots,6, \tag{25}$$

where $\mathcal{L}_i$ is the Lie screw of the ith limb that is computed by means of the composed Lie products as follows:

$$\begin{aligned}\mathcal{L}_i=&\left[{}_0\omega^i_1\,{}^0\$^1_i\quad {}_1\omega^i_2\,{}^1\$^2_i+\cdots+{}_5\omega^i_6\,{}^5\$^6_i\right]+\cdots\\&+\left[{}_4\omega^i_5\,{}^4\$^5_i\quad {}_5\omega^i_6\,{}^5\$^6_i\right]\end{aligned} \tag{26}$$

in which the brackets $[\cdots]$ denote the Lie product of two six-dimensional vectors.

Equation (25) can be rewritten in a more compact form as follows:

$$\mathbf{J}_i\dot{\Omega}_i={}^0\boldsymbol{A}^1_{P1}-\mathcal{L}_i, \tag{27}$$

where $\dot{\Omega}_i=[{}_0\dot{\omega}^i_1;{}_1\dot{\omega}^i_2;{}_1\dot{\omega}^i_2;{}_2\dot{\omega}^i_3;{}_3\dot{\omega}^i_4;{}_4\dot{\omega}^i_5;{}_5\dot{\omega}^i_6]^{\mathrm{T}}$ is a matrix containing the joint acceleration rates of the ith leg. Furthermore, the joint acceleration rates $\{{}_0\dot{\omega}^1_1=\ddot{q}_1,\,{}_0\dot{\omega}^2_1=\ddot{q}_2,\,{}_2\dot{\omega}^1_3=\ddot{q}_4,\,{}_2\dot{\omega}^2_3=\ddot{q}_5,\,{}_0\dot{\omega}^1_1=\ddot{q}_6\}$ are the generalized accelerations of the base module.

The inverse acceleration analysis (IAA) consists of finding the joint acceleration rates of the limbs of the base module given the accelerator of platform 1 with respect to platform 0. The IAA is computed directly from Eq. (27) as

$$\dot{\Omega}_i=\mathbf{J}_i^{-1}\left({}^0\boldsymbol{A}^1_{P1}-\mathcal{L}_i\right). \tag{28}$$

On the other hand, the forward acceleration analysis (FAA) consists of finding the reduced acceleration state ${}^0\boldsymbol{A}^1_{P1}$ of body 1 with respect to body 0 given a set of active joint acceleration rates $\{\ddot{q}_1,\ddot{q}_2,\ddot{q}_4,\ddot{q}_5,\ddot{q}_6\}$. Following the trend of the FVA, the systematic application of the Klein form between the reciprocal screws indicated in the FVA with both sides of expression (25), and casting into a matrix–vector form the equations thus derived, leads to

$$\mathrm{J}^{\mathrm{T}}\,\Delta\,{}^0\boldsymbol{A}^1_{P1}=\begin{bmatrix}\ddot{q}_1\left\{{}^3\$^4_1;{}^0\$^1_1\right\}+\left\{{}^3\$^4_1;\mathcal{L}_1\right\}\\ \ddot{q}_2\left\{{}^3\$^4_2;{}^0\$^1_2\right\}+\left\{{}^3\$^4_2;\mathcal{L}_2\right\}\\ \ddot{q}_4+\left\{{}^5\$^6_4;\mathcal{L}_4\right\}\\ \ddot{q}_5+\left\{{}^5\$^6_5;\mathcal{L}_5\right\}\\ \ddot{q}_6+\left\{{}^5\$^6_6;\mathcal{L}_6\right\}\\ \left\{{}^5\$^6_1;\mathcal{L}_1\right\}\end{bmatrix}. \tag{29}$$

Furthermore, since the accelerator satisfies the conditions of a helicoidal vector field, see Gallardo-Alvarado *et al.*,[44] it is possible to obtain the accelerator of platform 1 with respect to platform 0 taking the origin O of the global reference frame OXYZ as the reference pole as follows:

$${}^0\boldsymbol{A}^1_O=\begin{bmatrix}{}^0\dot{\boldsymbol{\omega}}^1\\ \mathrm{D}\left({}^0\boldsymbol{A}^1_{P1}\right)+{}^0\dot{\boldsymbol{\omega}}^1\times\boldsymbol{r}_{O/P1}\end{bmatrix}, \tag{30}$$

where D denotes the dual part of the indicated six-dimensional vector. Thereafter, the procedure to compute the accelerator can be repeated systematically for obtaining the accelerator of any moving platform k of the SHRM with respect to the fixed platform, ${}^0\boldsymbol{A}^k_O$. In fact, see Rico *et al.*,[48] it is possible to write

$$\begin{aligned}{}^0\boldsymbol{A}^k_O=&{}^0\boldsymbol{A}^1_O+{}^1\boldsymbol{A}^2_O+\ldots+{}^{k-1}\boldsymbol{A}^k_O\\&+\left[{}^0\boldsymbol{V}^1_O\quad {}^1\boldsymbol{V}^2_O+\ldots+{}^{k-1}\boldsymbol{V}^k_O\right]\\&+\left[{}^1\boldsymbol{V}^2_O\quad {}^2\boldsymbol{V}^3_O+\ldots+{}^{k-1}\boldsymbol{V}^k_O\right]+\ldots\\&+\left[{}^{k-2}\boldsymbol{V}^{k-1}_O\quad {}^{k-1}\boldsymbol{V}^k_O\right]\quad k=1,2,\ldots,n,\end{aligned} \tag{31}$$

where each relative accelerator ${}^{k-1}\boldsymbol{A}^k_O(k=1,\ldots,n)$ is computed, using properly the corresponding reference frames, according to Eqs. (29) and (30).

Finally, once the reduced acceleration state of the output platform with respect to the fixed platform is computed, six-dimensional vector ${}^0\boldsymbol{A}^n_O=[{}^0\dot{\boldsymbol{\omega}}^n;{}^0\boldsymbol{a}^n_O-{}^0\boldsymbol{\omega}^n\times{}^0\boldsymbol{v}^n_O]^{\mathrm{T}}$, the linear acceleration of the center of the output platform is obtained combining elementary kinematics and the properties of a helicoidal vector field as follows:

$${}^0\boldsymbol{a}^n_o=\mathrm{D}\left({}^0\boldsymbol{A}^n_O\right)+{}^0\dot{\boldsymbol{\omega}}^n\times\boldsymbol{r}_{o/O}+{}^0\boldsymbol{\omega}^n\times\left({}^0\boldsymbol{v}^n_o\right). \tag{32}$$

5. Numerical Example

In this section the kinematics of an SHRM built with four modules is presented. The parameters, using SI units, for the base module and its home position are listed in Table I.

The home position of the base module is repeated for each module by increasing in $n_{mod}h(n_{mod}=2,3,4)$ times the coordinate along the Y-axis. Keeping this in mind, the

https://doi.org/10.1017/S0263574710000421 Published online by Cambridge University Press

Table I. Parameters and home position of the base module.

$A_1 = (0.05, 0.0, 0.0)$, $A_2 = (-0.025, 0, -0.0433)$
$A_3 = (-0.025, 0, 0.0433)$, $S'_4 = (0.025, 0, -0.0433)$
$S'_5 = (-0.05, 0.0, 0.0)$, $S'_6 = (0.025, 0, 0.0433)$
$S_4 = (0.025, 0, -0.02)$, $S_5 = (-0.029, 0.05, -0.011)$
$S_6 = (0.004, 0.05, 0.03165)$
$D_1 = (0.025, 0.0175, -0.025)$, $D_2 = (-0.034, 0.0175, -0.0091)$
$D_3 = (0.009, 0.0175, 0.034)$, $C' = (0, 0, 0)$, $C = (0, 0.05, 0)$
$d_1 = d_2 = d_3 = e_1 = e_2 = e_3 = 0.0353$, $h = 0.05$, $r = 0.032$

Table II. Coefficients of the generalized coordinates.

j	C_1^j	C_2^j	C_4^j	C_5^j	C_6^j
1	0.1	−0.125	−0.0025	0.01	−0.005
2	−0.25	0.1	0.005	−0.01	0.005
3	0.125	−0.125	0.0035	−0.01	0.0075
4	0.1	−0.125	−0.0025	0.01	−0.0075

resulting home position of the SHRM is depicted in Fig. 1. Furthermore, the actuable joints are affected by periodical functions of the form $C_i^j \sin(t)$, where C_i^j is the coefficient associated with the ith generalized coordinate in the jth module; these coefficients are given in Table II. With these data, the exercise consists of finding the time history of the angular and linear kinematic properties of the center of the output platform with respect to the fixed platform, expressed in the reference frame OXYZ.

As expected, due to the periodical functions, three-dimensional undulatory motions are generated in the SHRM, animations in mpg format are available for this example, and the most representative numerical results obtained for it are given in Fig. 5. Finally, the numerical results obtained via screw theory are compared with results generated with the aid of special software such as ADAMS©.

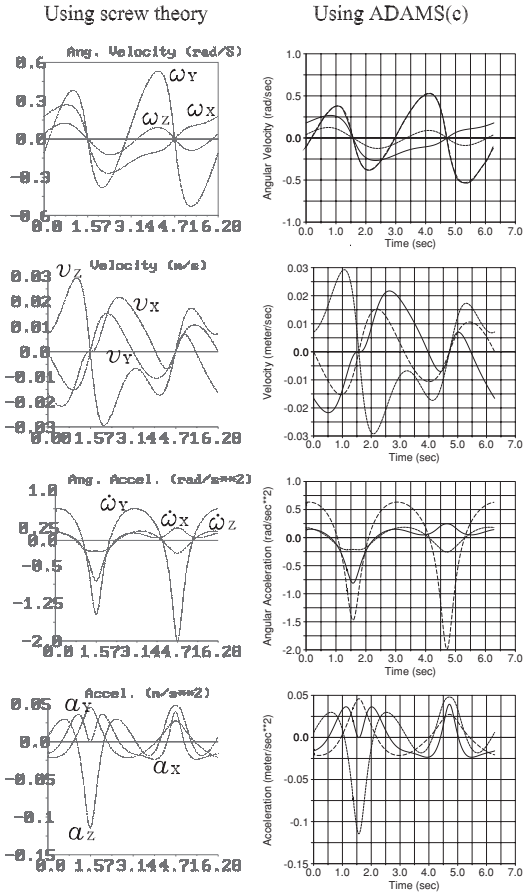

Fig. 5. Time history of the kinematics of the center of the output platform.

6. Conclusions

In this paper, a new spatial hyper-redundant manipulator is introduced. The proposed spatial mechanism is built with an optional number of tandem-assembled identical modules. The base module brings the following features:

- Decoupled architecture, which is a combination of a spherical parallel manipulator with a redundant planar parallel manipulator for controlling the orientation and position, respectively, of one platform with respect to the other.
- The forward displacement analysis is presented in a semi-closed form solution. All the feasible locations of one platform, with respect to the other, can be calculated given the generalized coordinates. The solution of the FDA, a challenging intensive task for most parallel manipulators, does not require the implementation of a numerical technique such as the Newton–Raphson method. Furthermore, the position and orientation are, conveniently, computed separately.
- A redundant limb allows the module to avoid/escape from possible singular configurations.
- Simple and compact expressions for solving the velocity and acceleration analyses are derived here by applying the concept of reciprocal screws via the Klein form of the Lie algebra $e(3)$, which is isomorphic to screw theory.
- The base module is a non-overconstrained parallel manipulator and therefore does not require additional conditions of manufacture like concurrent revolutes.

The kinematic analysis, expressed in a global reference frame attached at the fixed platform, of the SHRM is carried out using recursively the results obtained for the base module.

Among typical applications of spatial hyper-redundant manipulators such as devices for high manipulability in the context of space robotics and obstacle avoidance ability, biomechanical applications are available for this new SHRM, which was inspired by the motions of worms; in fact, the similarity of the proposed SHRM with the spine is indisputable. In that way, it is opportune to mention that considerable and valuable literature is reported day by day in order to approach the kinematic analysis of the spine; however, van Dieën *et al.*[49] pointed out that changes in the movement pattern at the level of a single or a number of motion segments of the spine will be missed by any method that treats the trunk, like the spine, as a rigid segment. Using the proposed SHRM, the spine can be modeled as several parallel manipulators, with autonomous motions, assembled in series connection, which without doubt is a viable option.

https://doi.org/10.1017/S0263574710000421 Published online by Cambridge University Press

Finally, an example, whose numerical results are validated with the aid of special software such as ADAMS© is provided.

Acknowledgments
This work was supported by the National Council of Science and Technology, Conacyt, of Mexico.

References

1. G. S. Chirikjian, Theory and Applications of Hyper-Redundant Robotic Manipulators *Ph.D. Thesis* (California Institute of Technology, 1992).
2. T. Ionescu, "Standardization of terminology," *Mech. Mach. Theory* **38**, 607–682 (2003).
3. G. S. Chirikjian and J. W. Burdick, "Kinematics of Hyper-Redundant Locomotion with Applications to Grasping," *Proceedings IEEE International Conference on Robotics and Automation,* Sacramento, CA (1991) pp. 720–727.
4. J. S. Pettinato and H. E. Stephanou, "Manipulability and Stability of a Tentacle Based Robot Manipulator," *Proceedings of the IEEE International Conference on Robotics and Automation*, Scottsdale, AZ (1989), vol. 1, pp. 458–463.
5. E. Paljug, T. Ohm and S. Hayati, "The JPL Serpentine Robot: A 12-DOF System for Inspection," *Proceedings of the IEEE International Conference on Robotics and Automation,* Nagoya, Japan (1995), pp. 3143–3148.
6. K. J. Kyriakopoulos, G. Migadis and K. Sarrigeorgidis, "The NTUA snake: Design, planar kinematics and motion planning," *J. Robot. Syst.* **16**, 37–72 (1999).
7. M. W. Hanan and I. A. Walker, "Kinematics and the implementation of an elephantŠs trunk manipulator and other continuum style robots," *J. Robot. Syst.* **20**, 45–63 (2003).
8. K. Zimmermann and I. Zeidis, "Worm-like locomotion as a problem of nonlinear dynamics," *J. Theor. Appl. Mech.* **45**, 179–187 (2007).
9. K. Zimmermann, I. Zeidis, J. Steigenberger, C. Behn, V. Böhm, J. Popp, E. Kolev and V. A. Naletova, "Worm-Like Locomotion Systems (WLLS)—Theory, Control and Prototypes," **In**: *Climbing & Walking Robots, Towards New Applications* (H. Zhang, ed.) (Itech Education and Publishing, Vienna, Austria, 2007) pp. 429–456.
10. C. Behn and K. Zimmermann, "Worm-Like locomotion Systems at the TU Ilmenau," *Proceedings of the 12th IFToMM World Congress*, Besancon (2007).
11. M. M. Panjabi and A. A. White, "Basic biomechanics of the spine," *Neurosurgery* **7**, 76–93 (1980).
12. J. Dimnet, A. Pasquet, M. H. Krag and M. M. Panjabi, "Cervical spine motion in the sagittal plane: Kinematic and geometric parameters," *J. Biomech.* **15**, 959–969 (1982).
13. S. Gracovetsky and H. Farfan, 1986 "The optimum spine," *Spine* **11**, 543.
14. J. Cholewicki and S. M. McGill, "Lumbar spine kinematics obtained from videofluoroscopy," *J. Biomech.* **25**, 801 (1992).
15. N. Yoganandan, F. Pintar, D. J. Maiman, J. Reinartz, A. Sances, S. J. Larson and J. F. Cusick, "Kinematics of the lumbar spine following pedicle screw plate fixation," *Spine* **18**, 504–512 (1993).
16. S. M. Levin, "The Importance of Soft Tissue for Structural Support of the Body," **In**: *Prolotherapy in the Lumbar Spine and Pelvis, Spine: State of the Art Reviews* (T. A. Dorman, ed.) (1995), vol. 9, issue 2, p. 357.
17. J. M. Willems, G. A. Jull and J. K.-F. Ng, "An in vivo study of the primary and coupled rotations of the thoracic spine," *Clin. Biomech.* **11**(6), 311–316 (1996).
18. M. J. Faber, H. C. Schamhardt and P. R. van Weeren, "Determination of 3D spinal kinematics without defining a local vertebral coordinate system," *J. Biomech.* **32**, 1355–1358 (1999).
19. T. Garcia and B. Ravani, "A biomechanical evaluation of whiplash using a multi-body dynamic model," *ASME J. Biomech. Eng.* **125**, 254–265 (2003).
20. H. Yoshikawa, T. Ishii, Y. Mukai, N. Hosono, H. Sakaura, Y. Nakajima, Y. Sato and K. Sugamoto, "Kinematics of the upper cervical spine in rotation: *In vivo* three-dimensional analysis," *Spine* **29**, E139–E144 (2004).
21. M. Ziddiqui, E. Karadimas, M. Nicol, F. W. Smith and D. Wardlaw, "Effects of X-stop device on sagittal lumbar spine kinematics in spinal stenosis," *J. Spinal Disorden Technol.* **19**, 328–333 (2006).
22. T. Ishii, Y. Mukai, N. Hosono, H. Sakaura, R. Fujii, Y. Nakajima, S. Tamura, M. Iwasaki, H. Yoshikawa and K. Sugamoto, "Kinematics of the cervical spine in lateral bending: *In vivo* three-dimensional analysis," *Spine* **31**, 155–160 (2006).
23. R. J. Konz, S. Fatone, R. L. Stine, A. Ganju, S. A. Gard and S. L. Ondra, "A kinematic model to assess spinal motion during walking," *Spine* **31**, E898–E906 (2006).
24. V. C. Chanceya, D. Ottaviano, B. S. Myers and R. W. Nightingale, "A kinematic and anthropometric study of the upper cervical spine and the occipital condyles," *J. Biomech.* **40**, 1953–1959 (2007).
25. K. P. Gill, S. J. Bennett, G. J. P. Savelsbergh and J. H. van Dieën, "Regional changes in spine posture at lift onset with changes in lift distance and lift style," *Spine* **32**, 1599–1604 (2007).
26. M. Jones, C. Holt and D. Franyuti, "Developing a methodology for the analysis of infant spine kinematics for the investigation of the shaken baby syndrome," *J. Biomech.* **41**, S355 (2008).
27. K. Iqbal and A. Roy, "A novel theoretical framework for the dynamic stability analysis, movement control, and trajectory generation in a multisegment biomechanical model," *ASME J. Biomech. Eng.* **131**, 011002 (2009).
28. S. J. Zhu, Z. Huang and M. Y. Zhao, "Feasible Human Spine Motion Simulators Based on Parallel Manipulators," **In**: *Parallel Manipulators, Towards New Applications* (H. Wu, ed.) (I-Tech Education and Publishing, Vienna, Austria, 2008) pp. 497–506.
29. A. Wolf, H. B. Brown, R. Casciola, A. Costa, M. Schwerin, E. Shamas and H. Choset, "A Mobile Hyper Redundant Mechanism for Search and Rescue Tasks," *Proceedings of the 2003 IEEE/RSJ International Conference on Intelligent Robots and Systems*, Las Vegas, Nevada (2003) pp. 2889–2895.
30. G. S. Chirikjian and J. W. Burdick, "A modal approach to hyper-redundant kinematics," *IEEE Trans. Robot. Autom.* **10**, 343–354 (1994).
31. G. S. Chirikjian and J. W. Burdick, "Kinematically optimal hyper-redundant manipulator configurations," *IEEE Trans. Robot. Autom.* **11**, 794–806 (1995).
32. J. W. Burdick, J. Radford and G. S. Chirikjian, "A 'sidewinding' locomotion gait for hyper-redundant robots," *Adv. Robot.* **9**, 195–216 (1995).
33. K. Wohlhart, "Displacement analysis of the general spherical Stewart platform," *Mech. Mach. Theory* **29**, 581–589 (1994).
34. J. Gallardo-Alvarado, "Kinematics of a hybrid manipulator by means of screw theory," *Multibody Syst. Dyn.* **14**, 345–366 (2005).
35. W. Li, F. Gao and J. Zhang, "R-CUBE, a decoupled parallel manipulator only with revolute joints," *Mech. Mach. Theory* **40**, 467–473 (2005).
36. G. Yang, I.-M. Chen, W. Chen and W. Lin, "Kinematic design of a six-dof parallel-kinematics machine with decoupled-motion architecture," *IEEE Trans. Robot.* **20**, 876–884 (2004).
37. M. R. Walker and J. P. Dickey, "New methodology for multi-dimensional spinal joint testing with a parallel robot," *Med. Biol. Eng. Comput.* **45**, 297–304 (2007).
38. S. J. Zhu, Z. Huang and M. Y. Zhao, "Singularity analysis for six practicable 5-DoF fully-symmetrical parallel manipulators," *Mech. Mach. Theory* **44**, 710–725 (2009).

39. C. Innocenti and V. Parenti-Castelli, "Direct position analysis of the Stewart platform mechanism," *Mech. Mach. Theory* **35**, 611–621 (1990).
40. L.-W. Tsai, *Robot Analysis* (John Wiley & Sons, New York, 1999).
41. J. Gallardo-Alvarado, R. Rodríguez-Castro and Md. N. Islam, "Analytical solution of the forward position analysis of parallel manipulators that generate 3-RS structures," *Adv. Rob.* **22**, 215–234 (2008).
42. J. Gallardo-Alvarado, C. R. Aguilar-Nájera, Casique-Rosas, L., L. Pérez-González and J. M. Rico-Martínez, "Solving the kinematics and dynamics of a modular spatial hyper-redundant manipulator by means of screw theory," *Multibody Syst. Dyn.* **20**, 307–325 (2008).
43. R. S. Ball, *A Treatise on the Theory of Screws* (Cambridge University Press, Cambridge, 1900) (reprinted 1998).
44. J. Gallardo-Alvarado, H. Orozco-Mendoza and R. Rodríguez-Castro, "Finding the jerk properties of multi-body systems using helicoidal vector fields," *Proc. Inst. Mech. Eng., Part* C*: J. Mech. Eng. Sci.* **222**, 2217–2229 (2008).
45. J. M. Rico and J. Duffy, "An Application of screw algebra to the acceleration analysis of serial chains," *Mech. Mach. Theory* **31**, 445–457 (1996).
46. G. Alici and B. Shirinzadeh, "Topology optimization and singularity analysis of a 3-SPS parallel manipulator with a passive constraining spherical joint," *Mech. Mach. Theory* **39**, 215–235 (2004).
47. J. M. Rico, J. Gallardo and J. Duffy, "A determination of singular configurations of serial non-redundant manipulators, and their escapement from singularities using Lie roducts," **In**: *Computational Kinematics '95* (J.-P. Merlet and Ravani, eds.) (Kluwer Academic Publishers, Niza, France, 1995) pp. 143–152.
48. J. M. Rico, J. Gallardo and J. Duffy, "Screw theory and higher order kinematic analysis of open serial and closed chains," *Mech. Mach. Theory* **34**, 559–586 (1999).
49. J. H. van Dieën, H. M. Toussaint, C. Maurice and M. Mientjes, "Fatigue-related changes in the coordination of lifting and their effect on low-back load," *J. Motor Behav.* **28**, 304–314 (1996).

https://doi.org/10.1017/S0263574710000421 Published online by Cambridge University Press